Coster-Kronig L-shell yield f_{23} of Dy, W, and Bi

Önder Şimşek
K. K. Education Faculty, Department of Physics, Atatürk University, 25240 Erzurum, Turkey
(Received 20 March 2000; published 19 October 2000)

The L-shell Coster-Kronig yield f_{23} has been measured for Dy, W, and Bi using an annular source double-reflection geometrical setup. Results for Dy, W, and Bi are 0.168 ± 0.013, 0.146 ± 0.008, and 0.135 ± 0.011, respectively. These results are compared with available theoretical calculations.

PACS number(s): 32.30.Rj

I. INTRODUCTION

A vacancy in an inner electron shell created, e.g., by photon or charged particle impact, is rapidly filled up by an electron from a higher-lying (sub)shell. Three different processes compete in the filling: The simplest one is the radiative one-electron decay in which one electron jumps ''down'' and the released energy is emitted as a fluorescence x ray. The other two are nonradiative processes: The so-called Auger process results from the mutual repulsion of two electrons in higher shells that causes one electron to jump down and the other to leave the atom carrying the excess energy as kinetic energy. The so-called Coster-Kronig decay is a special Auger process in which an initial vacancy is transferred to a higher subshell of the same shell. The relative probabilities of the various processes of vacancy filling are called (vacancy) yields.

Accurate experimental values of L-subshell fluorescence and Coster-Kronig yields also are important in many practical applications, ranging from elemental analysis by x-ray emission techniques to basic studies of nuclear and atomic processes leading to emission of x rays and Auger electrons, such as electron capture, internal conversion, and ionization cross-section measurements.

Three sets of values of L_i-subshell fluorescence yields ω_i and Coster-Kronig transitions probabilities f_{ij} are available in the literature. The first set, compiled by Krause [1], consist of semiempirically fitted values of ω_i and f_{ij} for all elements in the atomic range $12 \leqslant Z \leqslant 110$. The second set of these parameters, based on the relativistic Dirac-Hartree-Slater model, was tabulated in Ref. [2] for 25 elements in the atomic range $18 \leqslant Z \leqslant 100$. The third set of these values, using radiative and nonradiative transition rates based on the relativistic Dirac-Hartree-Slater model for all elements in the atomic range $25 \leqslant Z \leqslant 96$, was evaluated by Puri *et al.* [3]. A review of the literature [4–9] shows that a number of experimental studies on Coster-Kronig and fluorescence yields of L subshells were reported. In recent years, a systematic study of L-shell fluorescence yields for different elements, in the atomic region $56 \leqslant Z \leqslant 92$, was undertaken by us in Refs. [10–12].

In the present investigations, the Coster-Kronig probabilities f_{23} for Dy, W, and Bi, were deduced by measuring the L x rays emitted from the secondary targets excited by the K x rays of the elements used as primary targets. To obtain the L-shell Coster-Kronig yields f_{23} of Dy, W, and Bi, measurements are made using selective photoionization of the L_2 and L_3 subshells in these elements.

II. THEORETICAL ESTIMATION OF L X-RAY FLUORESCENCE CROSS SECTIONS

Case 1

Whenever the excitation energy (E) is less than the binding energy of the L_2 subshell but sufficient to excite the L_3 subshell, i.e., $B_{L_3} < E < B_{L_2}$, x-ray fluorescence cross sections for the $L\alpha$ x-ray line ($\sigma_{L\alpha}$) can be calculated using the relation

$$\sigma_{L\alpha} = \sigma_{L_3} \omega_3 F_{3\alpha}, \tag{1}$$

where σ_{L_3} is the photoelectric cross-section at the excitation energy, ω_3 is the L_3 subshell fluorescence yield, and $F_{3\alpha}$ is the fraction of L x rays originating from the L_3 transition that contribute to the $L\alpha$ peak.

Case 2

Whenever the excitation energy (E) is less than the binding energy of the L_1 subshell but sufficient to excite the L_2 subshell, i.e., $B_{L_2} < E < B_{L_1}$, x-ray fluorescence cross-sections for the $L\alpha$ x-ray line ($\sigma_{L\alpha}$) can be calculated using the relation

$$\sigma_{L\alpha} = (\sigma_{L_2} f_{23} + \sigma_{L_3}) \omega_3 F_{3\alpha}, \tag{2}$$

where f_{23} is the Coster-Kronig transition probability.

III. EXPERIMENTAL PROCEDURE AND DATA ANALYSIS

The experimental arrangement used in this study is shown in Fig. 1. Primary targets (P) are irradiated, in turn, with 59.54-keV γ rays from a filtered annular radioactive source (R) of ^{241}Am of intensity 100 m Ci which essentially emits monoenergetic (59.54-keV) γ rays, and the radiation emitted from the primary targets is collimated to fall on the secondary targets of Dy, W, and Bi. The L-shell fluorescent x rays emitted from secondary targets are recorded with Si(Li) x-ray detector (D), with resolution of ~160 eV at 5.9 keV, coupled to an ND 66B multichannel analyzer. The shielding in the arrangement is so arranged that the source can only ''see'' the primary target. The primary and secondary targets can see each other, and the detector can receive radiation only from the secondary target. The L-shell Coster-Kronig yields f_{23} of Dy, W, and Bi have been investigated by measuring the x-ray production cross sections of the $L\alpha$ group of L x rays by selective photoionization of L_2 and L_3 subshells

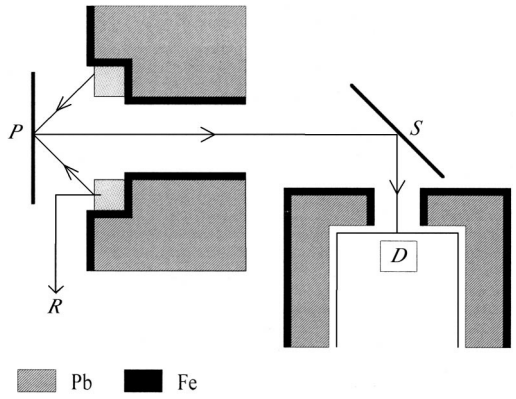

FIG. 1. Schematic diagram of the experimental setup: *R*, radiation source ^{241}Am (annular); *P*, primary target; *S*, secondary target; *D*, detector [Si(Li)].

in these elements. For selective photoionization of the L_3 subshell of Dy, W, and Bi, different primary targets were used. The primary target elements were chosen such that their $K\beta$ x rays [13] excited the L_3 subshells of Dy, W, and Bi, but did not excite the L_2 and L_1 subshells. Ni, Ge, and Rb $K\beta$ x rays were used to excite the L_3 subshells of Dy, W, and Bi, respectively. It can be seen that Ni, Ge, and Rb $K\alpha$ x rays [13] cannot excite the L_3 subshell of Dy, W, and Bi. For selective photoionization of the L_2 subshell of Dy, W, and Bi, Cu, As and Sr *K* conversion x rays were used. It can be seen that the $K\beta$ x rays of Cu, As, and Sr can photoionize the L_2 and higher subshell electrons in Dy, W, and Bi, respectively, and the L_1 subshell and *K* shell of these elements are not ionized. It was seen that Cu, As, and Sr $K\alpha$ x rays cannot excite the L_2 subshell, but can excite L_3 subshell of Dy, W, and Bi, respectively. The energy of γ rays scattered coherently and incoherently from the primary targets are greater than the L_1 threshold energy of all the secondary targets. γ rays scattered coherently and incoherently produce additional unwanted *L* x rays. The correction for the unwanted contribution of *L* x rays produced by scattered 59.54-keV γ rays was applied to *L* x rays counted in the detector by using an equivalent aluminum target in place of the primary target, as discussed in detail in an earlier paper [14]. Typical spectra of radiation emitted from Bi target when irradiated with radiation from primary targets of Rb and equivalent Al respectively, using the present experimental set-up are shown in Fig. 2(a) as spectra *A* and *B*. The difference spectrum *C* of the two spectra *A* and *B* (i.e., $C=A-B$) is also shown in Fig. 2(b).

Fluorescence cross sections for the $L\alpha$ x-ray line can be measured using the equation

$$\sigma_{L\alpha}=\frac{N_{L\alpha}}{I_0 G\varepsilon_{L\alpha}\beta_{L\alpha}t}. \tag{3}$$

Using Eqs. (1)–(3), the experimental *L*-shell Coster-Kronig yield f_{23} can be expressed as

$$f_{23}=\frac{N_{L\alpha}^2}{N_{L\alpha}^1}\frac{(I_0G)_1}{(I_0G)_2}\frac{\beta_{L\alpha}^1}{\beta_{L\alpha}^2}\frac{\sigma_{L_3}^1}{\sigma_{L_2}^2}-\frac{(I_0G)_3}{(I_0G)_2}\frac{\beta_{L\alpha}^3}{\beta_{L\alpha}^2}\frac{\sigma_{L_3}^3}{\sigma_{L_2}^2}, \tag{4}$$

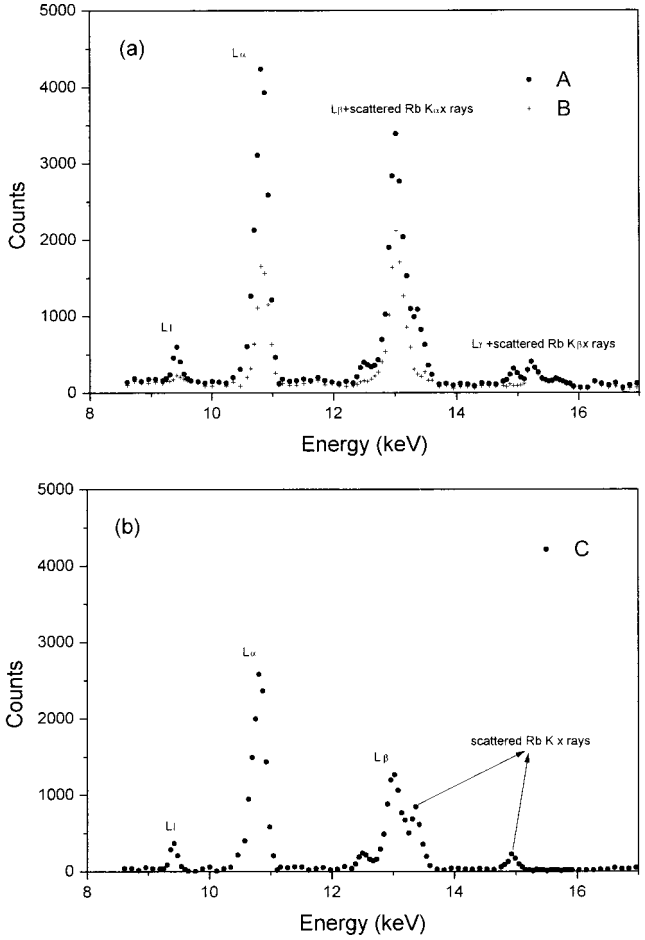

FIG. 2. (a) Typical spectra of the radiation from the Bi target recorded with a Si(Li) spectrometer. *A*, Rb primary target and Bi secondary target; *B*, equivalent Al primary target and Bi secondary target. (b) Net Bi *L* x-ray spectrum ($C=A-B$).

where $\sigma_{L_2}^i$ and $\sigma_{L_3}^i$ $(i=1,2,3)$ are the L_2- and L_3-subshell ionization cross sections, respectively. The numbers 1 and 2 correspond to the average $K\beta$ x-ray energy of primary targets which are used to excite L_3 and L_2 subshells of secondary targets, respectively. The number 3 corresponds to the weighted mean energy of the fluorescent *K* x rays of primary target elements which are used to excite the L_2 subshell of secondary targets. $N_{L\alpha}^i$ is the number of counts per unit time in the photopeak corresponding to the $L\alpha$ group of *L* x rays, and $(I_0G)_i$ is the intensity of the exciting radiation failing on the area of the secondary target visible to the detector. $\varepsilon_{L\alpha}$ is the efficiency of the detector at the average $L\alpha$ x-ray energy of the element, and *t* is the mass per unit area of the element in the secondary target. $\beta_{L\alpha}^i$ is the self-absorption correction factor, which accounts for the absorption in the secondary target material of the incident photons and of the emitted characteristic $L\alpha$ x rays.

In the present work, experimental f_{23} were evaluated using Eq. (4). The values of L_2- and L_3-subshell photoionization cross sections ($\sigma_{L_2}^i$ and $\sigma_{L_3}^i$) were taken from the tables of Scofield [15]. The self-absorption correction factor, $\beta_{L\alpha}^i$ was evaluated as described earlier [16]. $(I_0G)_1$ was deter-

mined by taking the *K* x-ray spectra of Co, Ga, and Br excited by Ni, Ge, and Rb $K\beta$ x rays, respectively. It can be seen that the $K\alpha$ x rays of Ni, Ge, and Rb cannot photoionize the *K*-shell electrons in Co, Ga, and Br, respectively. $(I_0G)_2$ was determined by measuring *K* x-ray yields from Ni, Ge, and Rb excited by the $K\beta$ x rays of Cu, As, and Sr, respectively. Cu, As, and Sr $K\alpha$ x rays cannot excite the *K* shells of Ni, Ge, and Rb, respectively. For determining the $(I_0G)_3$ value, an Fe foil was irradiated by the *K* x rays of Cu, As, and Sr, all of whose *K* x-ray lines can excite the *K* shell of Fe. $(I_0G)_i$ is evaluated using the relation

$$I_0G=\frac{N_{K\alpha}}{\sigma_{K\alpha}\varepsilon_{K\alpha}\beta_{K\alpha}t}, \tag{5}$$

where $N_{K\alpha}$, $\beta_{K\alpha}$, and $\varepsilon_{K\alpha}$ have the same meaning as in Eq. (3), except that they correspond to *K* x rays instead of *L* x rays. In these calculations, the theoretical values of *K* x-ray fluorescence cross sections ($\sigma_{K\alpha}$) were calculated using the equation

$$\sigma_{K\alpha}=\sigma_K(E)\omega_K f_{K\alpha}, \tag{6}$$

where $\sigma_K(E)$ is the *K*-shell photoionization cross section [15] at the excitation energy *E*, ω_K is the *K*-shell fluorescence yield from the tables of Hubbell *et al.* [17], and $f_{K\alpha}$ is the fractional x-ray emission rate for $K\alpha$ x rays and is defined as

$$f_{k\alpha}=\left(1+\frac{I_{K\beta}}{I_{K\alpha}}\right)^{-1}, \tag{7}$$

where $I_{K\beta}/I_{K\alpha}$ is the $K\beta$ to $K\alpha$ x-ray intensity ratio [18]. The detector efficiency was measured using ^{241}Am, ^{133}Ba, and ^{54}Mn radioisotope testing sources, as described earlier [19].

TABLE I. f_{23} measurements of Dy, W, and Bi.

Atomic number (Z)	Present values	Theoretical values		
		Ref. [1]	Ref. [2]	Ref. [3]
66 Dy	0.168 ± 0.013	0.143	-	0.155
74 W	0.146 ± 0.008	0.133	0.139	0.140
83 Bi	0.135 ± 0.011	0.113	-	0.121

IV. RESULT AND DISCUSSION

The measured values of the Coster-Kronig probability f_{23} for Dy, W, and Bi are listed in Table I. The overall error in the measured values is estimated to be 8%. This error is attributed to the uncertainties in the different parameters used to deduce f_{23} values [Eq. (4)], namely, the error in the area evaluation under the *L* x-ray peak ($\leqslant$5%), in the absorption correction factor ($\leqslant$3%), in the I_0G factor ($\cong$4–6 %), and other systematic errors ($\leqslant$4%).

For comparison the theoretical values of f_{23}, based on the relativistic Dirac-Hartree-Slater model, are given in Table I. The values of ω_i and f_{ij}, based on RDHS [2], are available for the limited number of elements only in the range $18\leqslant Z\leqslant 100$. The semiemprical values of Krause [1] and the calculated values by Puri *et al.* [3] are also given in Table I. In the calculation of Puri *et al.* [3], the ω_i and f_{ij} values for all the elements with the atomic region $25\leqslant Z\leqslant 96$ were calculated from the RDHS model based radiative emission rates of Scofield [18] and nonradiative emission rates of Chen, Creseman, and Mark [20]. It is clear from Table I that the present experimental results are in general agreement with the theoretical values.

[1] M. O. Krause, J. Phys. Chem. Ref. Data **8**, 307 (1979).
[2] M. H. Chen, B. Craseman, and H. Mark, Phys. Rev. A **24**, 177 (1981).
[3] S. Puri, D. Mehta, B. Chand, N. Sing, and P. N. Trehan, X-Ray Spectrom. **22**, 358 (1993).
[4] W. Jitschin, R. Stötzel, T. Papp, and M. Sarkar, Phys. Rev. A **59**, 3408 (1999).
[5] W. Jitschin, G. Materlik, U. Werner, and P. Funke, J. Phys. B **18**, 1139 (1985).
[6] M. Tan, R. A. Braga, and R. W. Fink, Phys. Scr. **37**, 62 (1988).
[7] D. G. Douglas, Can. J. Phys. **54**, 1124 (1976).
[8] J. M. Palms, R. E. Wood, P. V. Rao, and V. O. Kostroun, Phys. Rev. C **2**, 592 (1970).
[9] P. L. McGhee and J. L. Campbell, J. Phys. B **21**, 2295 (1988).
[10] Ö. Şimşek, O. Doğan, Ü. Turgut, and M. Ertuğrul, Radiat. Phys. Chem. **54**, 229 (1999).
[11] Ö. Şimşek, O. Doğan, Ü. Turgut, M. Ertuğrul, and H. Erdoğan, X-Ray Spectrom. **28**, 91 (1999).
[12] Ö. Şimşek, O. Doğan, Ü. Turgut, and M. Ertuğrul, Phys. Rev. A **58**, 1040 (1998).
[13] E. Strom and I. Israel, Nucl. Data, Sect. A **7**, 565 (1970).
[14] K. S. Mann, K. S. Kahlon, H. S. Aulakh, N. Sing, R. Mittal, K. L. Allawdhi, and B. S. Sood, Pramana J. Phys. **37**, 293 (1991).
[15] J. H. Scofield (unpublished).
[16] Ö. Şimşek, Nucl. Instrum. Methods Phys. Res. B **160**, 7 (2000).
[17] J. H. Hubbell, T. N. Trehan, N. Sing, B. Chand, D. Mehta, M. L. Garg, R. R. Garg, S. Sing, and S. Puri, J. Phys. Chem. Ref. Data **23**, 339 (1994).
[18] J. H. Scofield, At. Data Nucl. Data Tables **14**, 121 (1974).
[19] G. Budak, A. Karabulut, Ö. Şimşek, and M. Ertuğrul, Instrum. Sci. Technol. **27**, 357 (1999).
[20] M. H. Chen, B. Creseman, and H. Mark, At. Data Nucl. Data Tables **24**, 13 (1979).